Mechanistic Studies on the Cytochrome P450-Catalyzed Dehydrogenation of 3-Methylindole

Gary L. Skiles† and Garold S. Yost*

Department of Pharmacology and Toxicology, 112 Skaggs Hall, University of Utah, Salt Lake City, Utah 84112

Received June 30, 1995[⊗]

The mechanism of 3-methyleneindolenine (3MEI) formation from 3-methylindole (3MI) in goat lung microsomes was examined using stable isotope techniques. 3MEI is highly electrophilic, and its production is a principal factor in the systemic pneumotoxicity of 3MI. Noncompetitive intermolecular isotope effects of $^{D}V = 3.3$ and $^{D}(V/K) = 1.1$ obtained after deuterium substitution at the 3-methyl position indicated either that hydrogen abstraction from the methyl group was not the initial rate-limiting step or that this step was rate-limiting and was masked by a high forward commitment and low reverse commitment to catalysis. An intramolecular isotope effect of 5.5 demonstrated that hydrogen atom abstraction was probably the initial oxidative and rate-limiting step of 3MI bioactivation or that deprotonation of an aminium cation radical, produced by one-electron oxidation of the indole nitrogen, was rate-limiting. However, a mechanism which requires deprotonation of the aminium cation radical is probably precluded by an unusual requirement for specific base catalysis at a site in the cytochrome P450 enzyme other than the heme iron. The pattern of ^{18}O incorporation into indole-3-carbinol from $^{18}O_2$ and $H_2{}^{18}O$ indicated that approximately 80% of the indole-3-carbinol was formed in goat lung microsomes by hydration of 3MEI. However, the inverse reaction, dehydration of indole-3-carbinol, did not significantly contribute to the formation of 3MEI. These results show that 3MEI was formed in a cytochrome P450-catalyzed dehydrogenation reaction in which the rate-limiting step was presumably hydrogen atom abstraction from the 3-methyl position. The ratio of the amounts of 3MEI to indole-3-carbinol formed (50:1) indicated that dehydrogenation of 3MI is an unusually facile process when compared to the dehydrogenation of other substrates catalyzed by cytochrome P450 enzymes.

The pulmonary toxicity of 3-methylindole (3MI)[1] is at least in part due to alkylation of cellular proteins by a dehydrogenation product of its cytochrome P450-catalyzed metabolism: 3-methyleneindolenine (**4**, Scheme 1; 3MEI). The structure of 3MEI was first inferred when a glutathione adduct was isolated from goat lung microsomal incubations of 3MI that were supplemented with glutathione (*1*). Studies showed that covalent binding of 3MI in goat lung microsomes was inversely proportional to the concentration of supplemented glutathione or cysteine in the reactions (*2*) and that the in vivo toxicity of 3MI was proportional to depletion of glutathione in goat (*3*) and rat lungs (*4*). Bioactivation of 3MI to 3MEI was also shown to occur in vivo when a mercapturic acid adduct that was produced subsequent to glutathione conjugation of 3MEI was excreted from animals treated with 3MI (*5*). 3MEI also reacts with protein thiols, as shown by the isolation of a cysteine adduct of 3MI from hydrolysates of goat and human microsomal proteins that were covalently bound to 3MI in a P450-catalyzed reaction (*6*). The formation of 3MEI by cytochrome P450 enzymes has also been demonstrated in incubations of 3MI in lysates of cell lines containing expressed enzymes from cloned human, rabbit, and mouse P450s (*7*). The cytochrome P450-mediated production of 3MEI was also shown in isolated rabbit lung cells (*8*), where addition of 1-aminobenzotriazole, a mechanism-based inhibitor of cytochrome P450 enzymes, essentially abolished the production of the glutathione adduct of 3MEI. Thus, the formation of 3MEI appears to be mediated by several cytochrome P450 enzymes from

Scheme 1. Possible Mechanisms of 3-Methyleneindolenine (4) Formation from 3-Methylindole (1) in Goat Lung Microsomes[a]

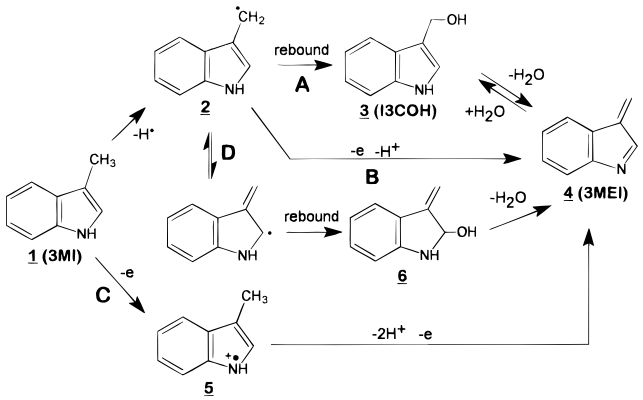

[a] Possible pathways are as follows: A, hydrogen atom abstraction, hydroxyl rebound, and dehydration of indole-3-carbinol (**3**); B, hydrogen atom abstraction followed by a second one-electron oxidation and proton loss; C, one-electron oxidation of the nitrogen followed by loss of a 3-methyl proton and a one-electron oxidation; and D, hydrogen atom abstraction and rearrangement of the radical followed by hydroxyl rebound and dehydration of the hemiaminal (**6**).

* Author to whom correspondence should be addressed.
† Present address: Biochemical and Investigative Toxicology, Department of Safety Assessment, WP45-319, Merck Research Laboratories, West Point, PA 19486.
⊗ Abstract published in *Advance ACS Abstracts,* December 15, 1995.
[1] Abbreviations: 3-methylindole, 3MI; 3-methyleneindolenine, 3MEI; indole-3-carbinol, I3COH; 3-[(*N*-acetyl-L-cystein-*S*-yl)methyl]indole, 3MINAC; 3-([$^2H_3$]methyl)indole, 3MI-d_3; 3-([$^2H_2$]methyl)indole, 3MI-d_2; *N*-acetyl-L-cysteine, NAC; cytochromes P450, P450; *N*-(trimethylsilyl)trifluoroacetamide, MSTFA.

0893-228x/96/2709-0291$12.00/0

several species. These and other mechanistic and toxicological aspects of 3MI metabolism have been previously reviewed (*9*, *10*).

The mechanism by which 3MEI is formed from 3MI is unclear. The P450-catalyzed reaction, $3MI + 2e^- + 2H^+ + O_2 \rightarrow 3MEI + 2H_2O$, describes a net dehydrogenation, but 3MEI could be formed from indole-3-carbinol (**3**, I3COH) that undergoes *dehydration* to form 3MEI (Scheme 1, pathway A). Acid-catalyzed dehydration of I3COH is a facile process and has been the subject of extensive study because I3COH is present in cruciferous vegetables and is suspected to act as an anticarcinogen (ref 11 and references therein). I3COH is a product formed during the P450-catalyzed metabolism of 3MI in vitro (*8*), and indole-3-carboxylic acid, presumably derived from I3COH, is a major product of the in vivo metabolism of 3MI (*12*). The most simple and reasonable mechanism of I3COH formation is via hydrogen radical abstraction and hydroxyl rebound. The intermediary carbon-centered radical (**2**) that occurs during the formation of I3COH might also undergo a one-electron oxidation to directly form 3MEI (Scheme 1, pathway B) if enzymatic and chemical conditions favor such a reaction. Alternatively, I3COH may be formed by hydration of 3MEI.

A completely different process of 3MEI formation, wherein an electron is abstracted from the nitrogen in the initial step followed by loss of a proton and a one-electron oxidation, is also possible (Scheme 1, pathway C). Such a mechanism is reasonable because 3MI has been shown to have a one-electron reduction potential of 1.05V (vs H) in studies where the nitrogen-centered cation radical was presumed to be the product of the one-electron oxidation of 3MI by perchlorate radical (*13*).

When cytochromes P450-catalyzed monooxygenations of xenobiotics occur at carbon atoms adjacent to, or conjugated with, nitrogen atoms, several lines of evidence have shown that the reactions proceed via an initial one-electron oxidation of the nitrogen followed by loss of the α or γ protons which are rendered more acidic by the aminium radical (*14*, *15*). After rearrangement of the radical to the α or γ carbon, hydroxyl rebound can occur to give a rearranged monooxygenated product. In lieu of hydroxyl rebound, abstraction of a second electron to yield a dehydrogenation product could also occur, particularly when the hydrogen is lost from the γ-position. The monooxygenated and dehydrogenated products could also be formed via an initial abstraction of the α or γ hydrogens; however, low kinetic deuterium isotope effects typically observed in these reactions have been interpreted to mean that nitrogen oxidation and not hydrogen abstraction is the initial step in the reaction.

The studies reported herein probed the different possible mechanisms for the formation of 3MEI and I3COH by determining the kinetic deuterium isotope effects in 3MEI and I3COH formation, and by measuring the incorporation of ^{18}O from $^{18}O_2$ and $H_2{}^{18}O$ into I3COH. The results demonstrate that (1) there is a high intramolecular deuterium isotope effect in the formation of 3MEI that may be due to a rate-limiting step of either hydrogen atom or aminium radical proton abstraction, (2) the majority of I3COH is formed by hydration of 3MEI, and (3) the ratio of dehydrogenation vs monooxygenation of 3MI that occurs in goat lung microsomes is unusually high when compared with other P450 substrates that also undergo dehydrogenation. Goat lung microsomes were used for these studies because goats are one of the most sensitive species to the toxic effects of 3MI.

Experimental Section

Chemicals. 3-Methylindole, indole-3-carboxylic acid, indole-3-carboxaldehyde, *N*-acetyl-L-cysteine (NAC), acetanilide, *p*-hydroxyacetanilide, benzoyl chloride (reagent grade), and $H_2{}^{18}O$ (95 atom %) were purchased from Aldrich Chemical Co. (Milwaukee, WI). Indole-3-carbinol was purchased from Sigma Chemical Co. (St. Louis, MO), and NADPH was purchased from United States Biochemical (Cleveland, OH). *N*-Methyl-*N*-(trimethylsilyl)trifluoroacetamide (MSTFA) and dry, silation-grade acetonitrile were purchased from Pierce Chemical Co. (Rockford, IL). $^{18}O_2$ (50 atom %) was obtained from Cambridge Isotope Laboratories (Woburn, MA). 3-[(*N*-Acetyl-L-cystein-*S*-yl)methyl]indole (3MINAC) was synthesized as previously described (*5*), and 3-([$^2H_3$]methyl)indole (3MI-d_3) and 3-([$^2H_2$]-methyl)indole (3MI-d_2) were synthesized by reduction of indole-3-carboxylic acid and indole-3-carboxyaldehyde, respectively, with $LiAlD_4$ according to a published method (*16*). Percent isotopic incorporation was determined by gas chromatography/mass spectrometry (*vide infra*) with the following results: 3MI-d_2 0.0079 (±0.0516)% d_0, 1.14 (±0.0501)% d_1, 98.5 (±0.0611)% d_2, 0.366 (±0.0351)% d_3; 3MI-d_3 0.0613 (±0.0089)% d_0, d_1 not detected, 2.10 (±0.0604)% d_2, 97.9 (±0.0626)% d_3. All other chemicals and reagents except those described below were purchased from local suppliers in the highest purity available.

Microsome Preparation. Goat lung and mouse liver microsomes (used for positive control experiments in the $^{18}O_2$-incorporation studies; described below) were prepared by standard centrifugal isolation procedures (*17*). Goat lungs were obtained from mature female goats. Goats were sedated with pentobarbital and killed by exsanguination. The lungs were perfused *in situ* with ice-cold 0.05 M phosphate buffer (pH 7.4) that contained 1 mM EDTA and 1.15% KCl, and then frozen at −80 °C. Mouse livers were obtained from male Swiss-Webster mice (SASCO, Omaha, NE) that were killed by cervical dislocation. The livers were rapidly removed and then minced in ice-cold 0.05 M Tris (Sigma) buffer (pH 7.4, determined at 25 °C) that contained 1.0 mM EDTA, 0.25 M sucrose, and 0.15 M KCl (buffer 1). Goat lung tissue was blended in a Waring blender in buffer 1 in a 4:1 buffer volume/tissue weight ratio. Blended goat lung tissue and minced mouse livers were homogenized with a Potter−Elvehjem homogenizer and then centrifuged at 9000*g* for 30 min to remove cellular debris. The supernatant was filtered through cheesecloth and then centrifuged at 105000*g* for 90 min. The microsomal pellets were resuspended in buffer 2 (identical to buffer 1 except that it did not contain KCl) in a 1:3 buffer volume/tissue weight ratio and then centrifuged a second time at 105000*g*, before they were again suspended in buffer 2 (1:3 dilution). The microsomal protein content was determined with a BSA Protein Assay Reagent Kit (Pierce), and the P450 content of the goat lung microsomes was determined from the dithionite-reduced difference spectra of carbon monoxide saturated microsomes as previously described (*18*). Microsomes were stored at −80 °C.

Deuterium Isotope Effect Incubations. Noncompetitive intermolecular deuterium-isotope effects were determined by incubating 0.05, 0.02, and 0.008 mM 3MI or 3MI-d_3 in goat lung microsomes (1.1 nmol of P450/mL), 1.0 mM NADPH, and 8.0 mM NAC in 0.05 M potassium phosphate buffer (pH 7.4) in a total volume of 3.0 mL at 37 °C. 3MEI was trapped with NAC to form 3MINAC because 3MEI is too reactive to quantify directly. Substrate was introduced in 10-μL volumes of ethanol, and incubations of each concentration of substrate were performed in triplicate. The reactions were stopped after 2.0 min by adding 3.0 mL of ice-cold acetonitrile. Denatured protein was precipitated by centrifugation, and then the supernatant was decanted and evaporated to about 1 mL *in vacuo*. The residue was brought to a volume of 1.5 mL with the starting HPLC mobile phase and analyzed directly (*vide infra*).

Intramolecular deuterium-isotope effects were determined by incubating 0.7 mM 3MI-d_2 under the identical conditions described above, except that the reactions were stopped after 8 min with 6.0 mL of ice-cold acetonitrile, and the total incubation volumes were 6.0 mL. After the protein pellets were precipi-

tated, the supernatants were decanted and evaporated under a stream of N_2 until the organic solvent was removed. The remaining aqueous solutions were extracted with Sep-Pak cartridges (Waters Associates, Millford, MA). The Sep-Pak cartridges were pre-wet with 15 mL of acetonitrile and then rinsed with 15 mL of 0.05 M aqueous ammonium carbonate (pH 6.8). The samples were placed on the cartridges which were then rinsed with 1.0 mL of 0.05 M aqueous ammonium carbonate and then eluted with 5.0 mL of acetonitrile. The eluate was stripped of solvent *in vacuo* then derivatized in 50 μL of a MSTFA/acetonitrile (1:1) solution by heating to 80 °C for 30 min in screw-cap sealed glass tubes.

Indole-3-carbinol Dehydration. Enzymatic and nonenzymatic dehydration of I3COH was determined by incubation of I3COH in the presence of 8.0 mM NAC for 30 min at 37 °C in 0.05 M potassium phosphate buffer (pH 7.4) under the following conditions: (1) 0.6 mM I3COH alone; (2) 0.6 mM I3COH, 1.0 mM NADPH, and goat lung microsomes; (3) 0.6 mM I3COH and goat lung microsomes; and (4) 0.01 mM I3COH, 1.0 mM NADPH, and goat lung microsomes. The final P450 concentration in those incubations that included microsomes was 1.1 nmol/mL. The samples were run in duplicate and were prepared for analysis as described for determination of the intermolecular isotope effect.

$^{18}O_2$ Incorporation. Incorporation of ^{18}O from molecular oxygen was determined by incubating 1.0 mM 3MI under the conditions described for the isotope effect experiments, except that in one set of incubations there was no NAC, in a total volume of 3.0 mL. The incubations were conducted in an air-tight, four-flask glass manifold system constructed so that it could be evacuated, flushed with N_2, and have $^{18}O_2$ (50 atom %) introduced from a lecture bottle. The incubation apparatus was generously loaned by Dr. William F. Trager, University of Washington. 3MI was incubated with goat lung microsomes in two of the flasks, and acetanilide was incubated with mouse liver microsomes in the other two flasks. Mouse liver microsomes were required for the hydroxylation of acetanilide because goat lung microsomes formed *p*-hydroxyacetanilide to such a small extent that it would have been very difficult to quantify the ^{18}O incorporation. After placing all of the incubation ingredients except for substrate into the system, the flasks were cooled on ice and the system was alternately evacuated and flushed with ultrapure N_2 at least 10 times. The 50 atom % ^{18}O oxygen was introduced, substrate was added through rubber septa, and the flasks were warmed to 37 °C and the contents stirred during a 30 min incubation. The reactions were stopped by immersing the flasks in a dry ice/acetone bath, and the flasks were removed from the manifold system. Three milliliters of ethyl acetate were placed on top of the frozen incubation solutions, and as they thawed, they were mixed to denature the protein and prevent any further metabolism in the presence of atmospheric O_2. The ethyl acetate layer was removed, and the aqueous solutions were extracted twice more with 3.0-mL aliquots of ethyl acetate. The pooled organic extracts were evaporated to dryness under an N_2 stream at ambient temperature and then derivatized in MSTFA/acetonitrile as described above.

$H_2{}^{18}O$ Incorporation. Incorporation of ^{18}O from $H_2{}^{18}O$ into I3COH was determined by incubating 3MI in a system in which the water was enriched with $H_2{}^{18}O$. Phosphate buffer was prepared by diluting 0.70 mL of 0.12 M phosphate buffer (pH 7.4) with 1.0 mL of $H_2{}^{18}O$ (95 atom %) to a final buffer concentration of 0.05 M. Duplicate incubations were set up by adding 67 μL of goat lung microsomes (final P450 concentration of 1.1 nmol/mL) to 433 μL of the buffer that had NADPH added to a final concentration of 1.0 mM. 3MI was added in 5 μL of ethanol, the flask contents were rapidly mixed, and 50-μL aliquots were immediately removed from each flask and placed in glass tubes on ice. The incubations were continued for 30 min at 37 °C and stopped by adding 500 μL of ice-cold ethyl acetate. The organic layers were removed, and the samples were extracted twice more with 500 μL of ethyl acetate. The extracts from each incubation were pooled and evaporated to dryness under a stream of N_2 before derivatization with MSTFA/acetonitrile (*vide supra*) for analysis by GC/MS. The heavy-isotope enrichment of water in the incubations was determined by ^{18}O incorporation into benzoic acid that was formed by hydrolysis of benzoyl chloride. The benzoyl chloride was added to aliquots that were removed from the incubations, rather than to the incubations themselves, because I3COH is unstable under acidic conditions. $H_2{}^{18}O$ enrichment of the incubations was determined individually to account for variations introduced when unlabeled water, present in the microsomes, was added. To each of the 50-μL aliquots that were removed prior to the incubations was added 5 μL of benzoyl chloride, and then they were immediately extracted three times with 50-μL portions of ethyl acetate. The extracts from each aliquot were pooled, evaporated to dryness under a stream of N_2, and derivatized with MSTFA for GC/MS analysis.

Liquid Chromatography. HPLC analysis was performed on a Beckman System Gold HPLC composed of a Model 126 solvent module and a Model 166 detector. Separation of analytes was achieved on a 250 × 4.6 mm Ultramex C_{18}, 5 μm HPLC column (Phenomenex, Torrance, CA) with a gradient solvent system that started at 20% 0.05 M ammonium acetate, pH 6.0, in acetonitrile and was ramped to 95% over 10.0 min and held there for 2.0 min before returning to 20% over 3.0 min. The UV detector monitored the absorbance at 280 nm, the λ_{max} of the benzenoid bands of I3COH and 3MINAC, and the metabolites were quantified by interpolation of their peak areas with standard curves established on each day of the analyses. Each sample was analyzed in triplicate.

Gas Chromatography/Mass Spectrometry. Isotopic enrichment of the deuterated 3MI substrates was determined with a VG Micromass 7070H gas chromatograph/mass spectrometer in the positive ion mode. Chromatography was performed on a 30 m wide bore DB-5 column (J&W Scientific, Folsom, CA) with a head pressure of 5 psi and a temperature program that was held at 100 °C for 1 min, ramped to 135 °C at 10 °C min^{-1}, and then held for 5 min before returning to 100 °C. The transfer line, re-intrant, and injector temperatures were 250, 200, and 250 °C, respectively. 3MI undergoes facile loss of a 3-methyl hydrogen under typical, 70 eV electron impact conditions. Such a loss would interfere with the determination of deuterium incorporation, so the ionization voltage was adjusted to 11 eV, the point where no loss of hydrogen from unlabeled 3MI was detected. In addition, the ion repeller was grounded to the source block to further protect from imparting ion energy sufficient to cause hydrogen loss. The ion abundance under these conditions was poor but adequate for the intended purpose. Ion channels corresponding to a mass range from M − 2 to M + 5 of 3MI-d_0 were monitored in SIM mode.

The ratios of metabolically produced isotopologs were determined by mass spectrometry with a Finnigan MAT 4500 gas chromatograph/mass spectrometer. The GC was fitted with a 30 m DB-5 microbore column with 0.25 μm film thickness (J&W Scientific). The carrier gas was hydrogen at a flow rate of ca. 30 m s^{-1}. The GC oven temperature profile started at 100 °C for 2.0 min and then was ramped at 10 °C min^{-1} for 13.0 min to 230 °C, then to 300 °C at 20 °C min^{-1}, before returning to 100 °C. The injector, ionizer, and transfer line temperatures were 270, 120, and 280 °C, respectively. Chemical ionization of the deuterated compounds was achieved using methane/ammonia (1:1) with (perfluorotributyl)amine enhancement (*19*), and ionization of the derivatized ^{18}O labeled I3COH, *p*-hydroxyacetanilide, and benzoic acid was accomplished by methane chemical ionization. The spectrometer was operated in the positive-ion mode, and each sample was analyzed in triplicate.

A full-scan spectrum of 3MINAC(TMS)$_3$ and I3COH(TMS)$_2$ standards ionized with CH_4/NH_3 showed that both compounds gave only one peak at m/z 202 corresponding to [MH − *N*-acetylcysteine(TMS)$_2$]$^+$ and [MH − OTMS]$^+$ for 3MINAC and I3COH, respectively; thus, the fragments of labeled metabolites would retain any deuterium atoms present in the compounds before fragmentation. The ion current for each ion of interest was enhanced during quantitation of the isotopolog ratios by

Table 1. Kinetic Constants and Calculated Inter- and Intramolecular Deuterium Isotope Effects

	intermolecular						intramolecular
metabolite	substrate[a]	K_m (mM)	V_{max}	^DV	V/K	$^D(V/K)$	^Dk
3MINAC	3MI-d_0	0.061 ± 0.0018	8.7 ± 0.25	3.3	143 ± 4.2	1.1	5.5 ± 0.5
	3MI-d_3	0.020 ± 0.0005	2.6 ± 0.065		133 ± 3.3		
13COH	3MI-d_0	0.10 ± 0.0042	1.3 ± 0.055	3.9	13 ± 0.55	1.1	4.8 ± 0.5
	3MI-d_3	0.029 ± 0.0013	0.34 ± 0.15		12 ± 0.53		

[a] Substrate used in intermolecular deuterium isotope effect experiments. 3MI-d_2 was the substrate used for the intramolecular isotope effect experiments.

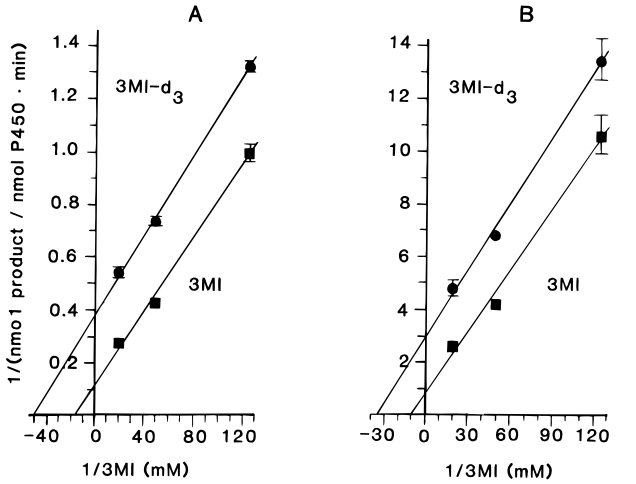

Figure 1. Lineweaver−Burk plots showing kinetic deuterium isotope effects on 3MINAC (A) and I3COH (B) formation from 3MI in goat lung microsomes. The substrates were unlabeled 3MI (3MI-d_0) and 3-($^3H_2$-methyl)indole (3MI-d_3). Error bars indicate the standard deviations of three analyses of three incubations at each concentration.

setting the mass spectrometer to a narrow scan width from m/z 200 to 210.

Ionization of standard I3COH(TMS)$_2$ with CH_4 gave the following spectrum [m/z, ion (rel abundance)]: 320, $[M + C_2H_5]^+$ (18); 292, MH^+ (63); 276, $[M - CH_3]^+$ (76); 230 (18); 202, [M − OTMS]$^+$ (100). For quantitation of the isotopolog ratios the $[M - CH_3]^+$ fragment was monitored because its abundance was higher than that of MH^+, because it retained the oxygen atom, and because it gave no M − 1 peak, which yielded more precise calculations of the ^{18}O incorporation. The spectrometer was set to scan m/z 274−286 to maximize the ion currents of each ion. The CH_4 CI spectrum of standard p-hydroxyacetanilide(TMS)$_2$ [m/z, ion (rel abundance): 324, $[M + C_2H_5]^+$ (24); 296, MH^+ (100); 280, $[M - CH_3]^+$ (94); 234 (19); 224 (10); 206, [M − OTMS]$^+$ (50)] indicated that monitoring the $[M - CH_3]^+$ peak would give nearly the same ion current as the base peak and it had virtually no M − 1 peak. The spectrometer was set to scan m/z 278−290 for quantitation of the isotopolog ratios. Ionization of standard benzoic acid(TMS) yielded the following spectrum: m/z 223, $[M + 29]^+$ (33); 195, MH^+ (100); 179, $[M - 15]^+$ (51); 142 (15); 110 (15). The MH^+ peak was monitored because it was the base peak and because it had only a minor M − 1 peak. The spectrometer was set to scan m/z 193−200 for quantitation of the isotopolog ratios.

Calculations. For the intermolecular deuterium-isotope experiments, the velocities of 3MINAC and I3COH production were calculated in terms of nmol of product (nmol of P450)$^{-1}$ min^{-1} and plotted on a Lineweaver−Burk graph to determine K_m and V_{max}. The overall catalytic efficiency (pseudo-second-order rate constant) was calculated as $k = V_{max}/K_m$ for each product, and then the isotope effect was expressed in the conventional manner as k_H/k_D.

Ratios of the deuterium and ^{18}O isotopologs were determined by the Brauman least-squares method (*20*) as further described by Korzekwa *et al.* (*21*). For the intramolecular deuterium-isotope experiments, the isotope effect was corrected for the statistical probability of hydrogen or deuterium removal by dividing the isotope effect, expressed as the ratios of the d_2 to d_1 metabolites, by 0.5 because the d_2/d_1 ratio would be 0.5 in the absence of an isotope effect. Deuterium incorporation into the labeled 3MI was sufficiently high that no further corrections of the data were performed. The value for ^{18}O incorporation into I3COH from $^{18}O_2$ was corrected for the ^{18}O incorporation into *p*-hydroxyacetanilide. Incorporation of ^{18}O into benzoic acid, formed from hydrolysis of benzoyl chloride by the $H_2{}^{18}O$ enriched water, served as the positive control and was used to correct the values for ^{18}O incorporation into I3COH from $H_2{}^{18}O$. Because oxygen exchange of carboxylic acids can occur in an aqueous environment (*22*), incorporation of two atoms of ^{18}O was evaluated in the analyses that measured ^{18}O incorporation into benzoic acid. The benzoic acid was extracted as rapidly as possible to minimize exchange, and no detectable exchange occurred as evidenced by the lack of any benzoic acid with two atoms of ^{18}O (data not shown).

Results

Intermolecular Deuterium Isotope Effects. The quantities of 3MINAC and I3COH produced from the various concentrations of 3MI used in the intermolecular deuterium-isotope effect experiments were used to construct the Lineweaver−Burk plots shown in Figure 1. In all cases the amount of 3MINAC formed was about 10 times that of the I3COH. No other known metabolites of 3MI were present to an appreciable extent (<5% of the 3MINAC) in the time frame of the incubations.

The metabolism kinetics for the formation of 3MINAC and I3COH from 3MI and 3MI-d_3 were calculated from Figure 1 and are shown in Table 1. In the formation of both compounds there was a decrease in V_{max} upon deuterium substitution that appears to indicate an isotope effect of between 3 and 4. When the isotope effect on V_{max}/K_m was compared, however, the apparent isotope effect on the pseudo-second-order rate constants was only about 1.1. These results are consistent with a simple model of enzyme kinetics described by Gillette (*23*) and shown in eq 1, where ES* is the substrate bound enzyme

$$E + S \underset{k_{-1}}{\overset{k_1}{\rightleftharpoons}} ES \underset{k_{-2}}{\overset{k_2}{\rightleftharpoons}} ES^* \xrightarrow{k_3} EP \xrightarrow{k_4} E + P \qquad (1)$$

with the activated perferryl−oxo complex and k_3 is the isotopically sensitive step. Northrop (*24*), Gillette (*23*), and others have shown that when there is a high commitment to catalysis ($k_{-2} \approx 0$), then V_{max} is directly proportional to k_3 (eq 2), and V_{max}/K_m is independent of k_3 (eq 3). The results of the intermolecular deuterium

$$\frac{V_m}{E_t} = \frac{1}{1/k_2 + 1/k_3 + 1/k_4} \qquad (2)$$

$$\frac{V_{max}}{K_m} = \frac{E_t k_1 k_2}{k_2 + k_{-1}} \qquad (3)$$

isotope effect experiments shown in Table 1 are in

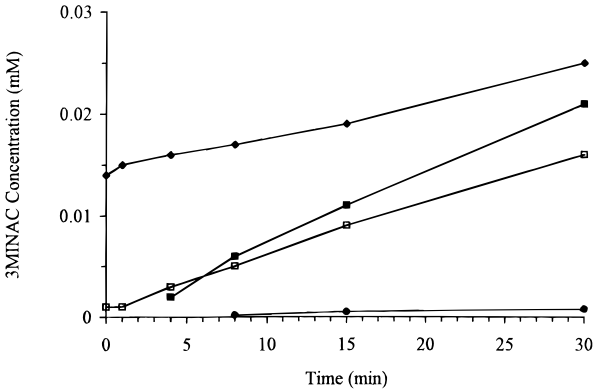

Figure 2. Time course of chemical and enzymatic dehydration of I3COH as determined by the amounts of 3MINAC formed from the methylene imine dehydration product. Incubation conditions: (♦) 0.6 mM I3COH, (−) goat lung microsomes, (−) NADPH; (■) 0.6 mM I3COH, (+) goat lung microsomes, (+) NADPH; (□) 0.6 mM I3COH, (+) goat lung microsomes, (−) NADPH; (●) 0.01 mM I3COH, (+) goat lung microsomes, (+) NADPH. Details of the incubation conditions are described in the Experimental Section.

agreement with this model and demonstrate that 3MI dehydrogenation is catalyzed by P450 enzymes in goat lung microsomes with a high commitment to catalysis, masking the intrinsic isotope effect on V_{max}/K_m.

Intramolecular Deuterium Isotope Effects. The low substrate concentrations used in the intermolecular isotope effect studies were necessary because the rate of product formation was nonlinear at higher concentrations. The substrate concentrations were significantly below the apparent K_ms for 3MINAC and I3COH formation, which led to uncertainty about the validity of the derived kinetic constants. Therefore, to verify an intrinsic kinetic deuterium isotope effect in the formation of 3MEI, the intramolecular deuterium isotope effect was also determined. The intramolecular deuterium isotope effect should not be susceptible to the masking observed in the isotope effect on V_{max}/K_m if there is free rotation about the methyl carbon−carbon bond. The rotation provides a mechanism that is effectively a branching pathway that relieves the high commitment to the incipient abstraction of a deuterium radical. The effect of metabolic branching on unmasking of kinetic deuterium isotope effects has been previously investigated experimentally by Jones *et al.* (*25*) and theoretically by Korzekwa *et al.* (*26*). The results shown in Table 1 support the hypothesis developed above because an intramolecular isotope effect of about 5 for I3COH formation and 5.5 for 3MINAC formation was observed. α-Secondary isotope effects were ignored in the calculations because they are typically small ($k_H/k_D \approx 1.2$) and they decrease the experimentally determined isotope effect. Therefore, the value obtained represents a minimum for the intrinsic isotope effect.

Dehydration of Indole-3-carbinol. The formation of 3MINAC from I3COH under various incubations conditions is shown in Figure 2. Incubation of relatively high concentrations (0.6 mM) of I3COH did not produce significant amounts of 3MINAC under any of the conditions tested. These experiments, however, did not address the possibility that a goat lung microsomal enzyme with a very low K_m may dehydrate I3COH to 3MEI; therefore, incubations were performed with a concentration of I3COH (0.01 mM) that more closely approximated the amount of I3COH formed from 3MI in the intermolecular isotope-effect experiments. As seen in Figure 2, incubation of a low concentration of I3COH produced negligible amounts of 3MINAC when compared to the total amount of 3MINAC produced during microsomal incubation of 3MI. Moreover, in the intermolecular isotope effect experiments, the concentration of 3MINAC formed from 3MI was always about 10 times that of I3COH, so the 3MINAC formed from the 0.01 mM concentration of I3COH in the dehydration experiments did not account for the large amounts of 3MINAC formed from 3MI in the isotope effect experiments. Small amounts of dehydration of I3COH occurred, but clearly, chemical and enzymatic dehydration are insignificant pathways of 3MEI formation.

Table 2. Incorporation of ^{18}O into I3COH from $^{18}O_2$ and $H_2{}^{18}O$ by Goat Lung Microsomes

			^{18}O incorporation[a] (%)	
exp.	^{18}O source	product	measured	corrected
1	$^{18}O_2$	APAP	49.1 ± 0.33	
		I3COH[b]	6.65 ± 0.65	14
2	$^{18}O_2$	APAP	49.8 ± 1.1	
		I3COH[c]	10.3 ± 4.2	21
3	$H_2{}^{18}O$	BA	42.9[d]	
		I3COH	36.6 ± 1.2	85
4	$H_2{}^{18}O$	BA	43.6 ± 0.95	
		I3COH	36.7 ± 1.2	84

[a] Percentage incorporated corrected for values of positive controls: acetaminophen (APAP) for $^{18}O_2$ in mouse liver microsomes and benzoic acid (BA) for $H_2{}^{18}O$ incorporation. [b] *N*-Acetylcysteine omitted from incubations. [c] *N*-Acetylcysteine added to incubations. [d] Mean of two measurements.

$^{18}O_2$ Incorporation in Indole-3-carbinol. Incorporation of molecular oxygen into I3COH, as determined by its ^{18}O content after incubation of 3MI in goat lung microsomes under a 50 atom % ^{18}O oxygen atmosphere, is shown in Table 2. Surprisingly, the relative proportion of I3COH formed by hydroxyl rebound in the absence of NAC was quite small. Indeed, the majority (87%) of the I3COH was formed by some other mechanism, probably hydration of 3MEI. The relatively large amount of I3COH formed by hydration of 3MEI in the absence of NAC could plausibly be explained by a process in which untrapped 3MEI reacted with water to an extent that would not normally occur if the 3MEI had been trapped with a thiol. To explore this possibility, the ^{18}O-incorporation experiment was repeated with NAC added to the microsomal incubation. In the presence of NAC, approximately the same proportion of the I3COH (21%) was formed by hydroxyl rebound (Table 2), indicating that, even in the presence of NAC, most of the I3COH (80%) was formed by a different pathway.

$H_2{}^{18}O$ Incorporation into Indole-3-carbinol. About 85% of I3COH in the absence of NAC was formed by a mechanism wherein oxygen that originated from water was incorporated into the molecule (Table 2). These results are in excellent agreement with the results of ^{18}O incorporation from $^{18}O_2$, also in the absence of NAC: 100% of the oxygen in I3COH could be accounted for having originated from either O_2 or H_2O. This is consistent with a hypothesis that most of the I3COH formed from 3MI in goat lung microsomal incubations resulted from hydration of the methylene imine.

Discussion

P450-supported dehydrogenation reactions are uncommon, but the importance of the reactions is increasingly

recognized as they have been demonstrated to occur during the metabolism of a number of compounds. Valproic acid (*27*), Δ^2-valproic acid (*28*), testosterone (*29*), butylated hydroxytoluene (*30*), ethyl carbamate (*31*), dihydropyridines (*32*), acetaminophen (*33*), flunisolide (*34*), and lovastatin (*35*) all undergo net dehydrogenations. The intermediacy of hydroxylated compounds that dehydrate has been suggested to occur with several of these compounds, and investigations have been conducted to ascertain the mechanism of net dehydrogenation. For example, early reports on the bioactivation of acetaminophen suggested the possibility that an *N*-hydroxylated intermediate dehydrated to form the *N*-acetyl-*p*-quinone imine that reacted with GSH and was believed to be at least partially responsible for covalent binding and toxicity. Studies on the chemistry of synthetic *N*-acetyl-*N*-hydroxy-*p*-aminophenol, however, demonstrated that this compound was relatively stable and was almost certainly not the precursor to the reactive intermediate. Later work provided persuasive evidence that two sequential one-electron oxidations by P450 was the mechanism by which the *N*-acetyl-*p*-quinone imine was formed (*33*).

The relatively high isotope effect observed in 3MI dehydrogenation is uncommon for the P450-catalyzed oxidation of a nitrogen-containing compound. While a catalytic hydrogen-abstraction mechanism might explain the isotope effect, reports that a high isotope effect can occur in nonenzymatic proton transfers from an aminium radical to a base (*36*) confound this interpretation. The compounds that can be most closely compared with 3MI are the dihydropyridines because they also lose an allylic hydrogen in their P450-catalyzed dehydrogenation (*15*, *32*). Deprotonation of dihydropyridine aminium radicals, formed by cytochrome P450 enzymes and peroxidases, has recently been reviewed (*37*). The pK_a of the dihydropyridine aminium radical was estimated to be ca. 3.5, a value similar to that reported for the 3MI aminium radical of 5.0 ± 0.1 (*13*). If 3MEI formation is initiated by *N*-oxidation, then like the dihydropyridines, specific $[Fe{-}O]^{2+}$ proton transfer is unlikely to occur because the acidic γ proton would be inaccessible when the substrate is oriented in the enzyme for oxidation of the nitrogen (*15*).

Equally probable, and perhaps more compelling because of its simplicity, is a mechanism in which P450-catalyzed hydrogen abstraction from the 3-methyl position occurs in lieu of nitrogen oxidation because of the orientation of the substrate in the binding site. Recent findings (*38*) indicate that amine dealkylations can indeed proceed via initial hydrogen atom abstraction, although it is uncertain whether these findings extend to the case of hydrogens that are γ to the amine nitrogen.

Stabilization of a radical metabolic intermediate is an emerging mechanistic explanation that can, in some cases, account for the occurrence of a dehydrogenation reaction in lieu of monooxygenation. In a report on the dehydrogenation of Δ^2-valproic acid (*28*), resonance stabilization of the allylic radical was invoked to explain the relatively high dehydrogenation to monooxygenation ratio, the "partition ratio". That same reasoning can be extended to the case of 3MI dehydrogenation initiated by hydrogen radical abstraction. The benzylic radical intermediate formed by hydrogen atom abstraction from the methyl group should be even more stable than an allylic radical and provide a greater opportunity for abstraction of the second electron from the substrate. In the report on the dehydrogenation of Δ^2-valproic acid, it was noted that no monooxygenation products of allylic rearrangement were found. This was presumably because the heme iron had access to the site of the second electron abstraction but not the rearranged radical. In the dehydrogenation of 3MI, the region of the substrate in which the radical is resonance stabilized and from where the second electron must be abstracted is the same. Thus, the lack of any monooxygenation products of benzylic rearrangement is not as easily explained. Indeed, a monooxygenation at a 2-carbon radical may occur, but the resulting 3-methylene hemiaminal (**6**) would probably undergo rapid dehydration to 3MEI (Scheme 1, pathway D).

Like other compounds that are dehydrogenated, monooxygenation at the site of hydrogen abstraction and dehydrogenation of 3MI both occurred; however, unlike many other examples, dehydrogenation of 3MI in goat lung microsomes is the predominant reaction. Compounds which can stabilize the intermediate by radical resonance typically have relatively high partition ratios, i.e., the ratio of dehydrogenation to monooxygenation. For instance, Δ^2-valproic acid had a partition ratio of about 0.5 (*28*), and the ratio for testosterone is about 1 (*29*). The ratios for other compounds such as valproate (*27*) and ethyl carbamate (*31*), in which no allylic stabilization of the radical is available, are 0.2 or less. The observed partition ratio for 3MI was about 10; moreover, the ^{18}O-incorporation studies showed that the majority of the I3COH was formed by hydration of 3MEI so that the actual proportion of dehydrogenation exceeded that of monooxygenation by over 50 times, a ratio that far exceeds other substrates.

The mechanism of 3MI dehydrogenation to form 3MEI most likely involves hydrogen atom abstraction as the rate-limiting step, but a mechanism requiring rate-limiting proton abstraction from an aminium cation radical cannot be eliminated at this time. However, the data presented here demonstrate that an unusually high isotope effect in the reaction distinguishes 3MI from similar nitrogen-containing substrates that also undergo P450-catalyzed dehydrogenations. A small amount of I3COH was shown to be formed by monooxygenation; however, dehydrogenation dominated to a remarkable extent, and the majority of I3COH was formed in goat lung microsomes via hydration of 3MEI. Indeed, the specificity of dehydrogenation rather than hydroxylation of 3MI represents an unique case of *preferential* P450-mediated dehydrogenation of a substrate to form a toxic electrophilic intermediate.

Acknowledgment. This work was supported by United States Public Health Service Grant HL13645 from the National Heart, Lung and Blood Institute and by a United States Public Health Service Research Career Development Award (Grant HL02119) to G.S.Y. We are grateful to Drs. Douglas E. Rollins and Roger L. Foltz, of the Center for Human Toxicology, and Mr. William Howald, of the University of Washington Department of Medicinal Chemistry, for providing mass spectrometry instrumentation.

References

(1) Nocerini, M. R., Yost, G. S., Carlson, J. R., Liberato, D. J., and Breeze, R. G. (1985) Structure of the glutathione adduct of activated 3-methylindole indicates that an imine methide is the electrophilic intermediate. *Drug Metab. Dispos.* **13**, 690−694.

(2) Nocerini, M. R., Carlson, J. R., and Yost, G. S. (1985) Glutathione adduct formation with microsomally activated metabolites of the pulmonary alkylating and cytotoxic agent, 3-methylindole. *Toxicol. Appl. Pharmacol.* **81**, 75−84.
(3) Nocerini, M. R., Carlson, J. R., and Breeze, R. G. (1983) Effect of glutathione status on covalent binding and pneumotoxicity of 3-methylindole in goats. *Life Sci.* **32**, 449−458.
(4) Adams, J. D., Laegreid, W. W., Huijzer, J. C., Hayman, C., and Yost, G. S. (1988) Pathology and glutathione status in 3-methylindole-treated rodents. *Res. Commun. Chem. Pathol. Pharmacol.* **60**, 323−335.
(5) Skiles, G. L., Smith, D. J., Appleton, M. L., Carlson, J. R., and Yost, G. S. (1991) Isolation of a mercapturate adduct produced subsequent to glutathione conjugation of bioactivated 3-methylindole. *Toxicol. Appl. Pharmacol.* **108**, 531−537.
(6) Ruangyuttikarn, W., Skiles, G. L., and Yost, G. S. (1992) Identification of a cystinyl adduct of oxidized 3-methylindole isolated from goat lung and human liver microsomal proteins. *Chem. Res. Toxicol.* **5**, 713−719.
(7) Thornton-Manning, J. R., Appleton, M. L., Gonzalez, F. J., and Yost, G. S. (1996) Metabolism of 3-methylindole by vaccinia-expressed cytochrome P450 enzymes: correlation of 3-methyleneindolenine formation and protein-binding. *J. Pharmacol. Exp. Ther.* (in press).
(8) Thornton-Manning, J. R., Nichols, W. K., Manning, B. W., Skiles, G. L., and Yost, G. S. (1993) Metabolism and bioactivation of 3-methylindole by Clara cells, alveolar macrophages and subcellular fractions from rabbit lungs. *Toxicol. Appl. Pharmacol.* **122**, 182−190.
(9) Yost, G. S. (1989) Mechanisms of 3-methylindole pneumotoxicity. *Chem. Res. Toxicol.* **2**, 273−279.
(10) Yost, G. S., Buckpitt, A. R., Roth, R. A., and McLemore, T. L. (1989) Contemporary issues in toxicology: Mechanisms of lung injury by systemically administered chemicals. *Toxicol. Appl. Pharmacol.* **101**, 179−185.
(11) Gross, K. R., and Bjeldanes, L. F. (1992) Oligomerization of indole-3-carbinol in aqueous acid. *Chem. Res. Toxicol.* **5**, 188−193.
(12) Smith, D. J. Skiles, G. L., Appleton, M. L., Carlson, J. R., and Yost, G. S. (1993) Metabolic fate of 3-methylindole in goats and mice. *Xenobiotica* **23,** 1025−1044.
(13) Merenyi, G., Lind, J., and Shen, X. (1988) Electron transfer from indoles, phenol, and sulfite (SO_3^{2-}) to chlorine dioxide ($ClO_2^{\bullet}$). *J. Phys. Chem.* **92**, 134−137.
(14) Ortiz de Montellano, P. R. (1989) Cytochrome P-450 catalysis: radical intermediates and dehydrogenation reactions. *Trends Pharmacol. Sci.* **10**, 354−359.
(15) Okazaki, O., and Guengerich, F. P. (1993) Evidence for specific base catalysis in *N*-dealkylation reactions catalyzed by cytochrome P-450 and chloroperoxidase. *J. Biol. Chem.* **268**, 1546−1552.
(16) Leete, E., and Marion, L. (1953) The hydrogenolysis of 3-hydroxymethylindole and other indole derivatives with lithium aluminum hydride. *Can. J. Chem.* **31**, 775−784.
(17) Ruangyuttikarn, W., Appleton, M. L., and Yost, G. S. (1991) Metabolism of 3-methylindole in human tissues. *Drug Metab. Dispos. 19*, 977−984.
(18) Johannesen, K. A. M., and DePierre, J. W. (1978) Measurement of cytochrome P-450 in the presence of large amounts of contaminating hemoglobin and methemoglobin. *Anal. Biochem.* **86**, 725−732.
(19) Levandoski, P., Straub, K., Shah, D., DeMarinis, R., and de May, C. (1986) High sensitivity assay for the α_2 antagonist 6-chloro-3-methyl-2,3,4,5-tetrahydro-1*H*-3-benzazepine and its desmethyl metabolite in plasma using gas chromatography mass spectrometry with ammonia/CCl_4 chemical ionization. *Biomed. Environ. Mass Spectrom.* **13**, 523−530.
(20) Brauman, J. I. (1966) Least squares analysis and simplificationof multi-isotope mass spectra. *Anal. Chem.* **38**, 607−610.
(21) Korzekwa, K., Howald, W. N., and Trager, W. F. (1990) The use of Brauman's least squares approach for the quantification of deuterated chlorophenols. *Biomed. Mass. Spectrom.* **19**, 211−217.
(22) Murphy, R. C., and Clay, K. L. (1990) Preparation of labeled molecules by exchange with oxygen-18 water. *Methods Enzymol.* **193**, 338−348.
(23) Gillette, J. R. (1990) Insights into deuterium isotope effects on the metabolism of steroid hormones and foreign compounds by cytochrome P-450 enzymes. *Life Sci.* **49**, 1−14.
(24) Northrop, D. B. (1982) Deuterium and tritium kinetic isotope effects on initial rates. *Methods Enzymol.* **87**, 607−625.
(25) Jones, J. P., Korzekwa, K. R., Rettie, A. E., and Trager, W. F. (1986) Isotopically sensitive branching and its effect on the observed intramolecular isotope effects in cytochrome P-450 catalyzed reactions: A new method for the estimation of intrinsic isotope effects. *J. Am. Chem. Soc.* **108**, 7074−7078.
(26) Korzekwa, K. R., Trager, W. F., and Gillette, J. R. (1989) Theory for the observed isotope effects from enzymatic systems that form multiple products via branched reaction pathways: Cytochrome P-450. *Biochemistry* **28**, 9012−9018.
(27) Rettie, A. E., Rettenmeier, A. W., Howald, W. N., and Baillie, T. A. (1987) Cytochrome P-450-catalyzed formation of Δ^4-VPA, a toxic metabolite of valproic acid. *Science* **235**, 890−893.
(28) Kassahun, K., and Baillie, T. A. (1993) Cytochrome P-450-mediated dehydrogenation of 2-*n*-propyl-2(E)-pentenoic acid, a pharmacologically-active metabolite of valproic acid, in rat liver microsomal preparations. *Drug Metab. Dispos.* **21**, 242−248.
(29) Korzekwa, K. R., Trager, W. F., Nagata, K, Parkinson, A., and Gillette, J. R. (1990) Isotope effect studies on the mechanism of the cytochrome P-450IIA1-catalyzed formation of Δ^6-testosterone from testosterone. *Drug Metab. Dispos.* **18**, 974−979.
(30) Bolton, J. L., and Thompson, J. A. (1991) Oxidation of butylated hydroxytoluene to toxic metabolites, factors influencing hydroxylation and quinone methide formation by hepatic and pulmonary microsomes. *Drug Metab. Dispos.* **19**, 467−472.
(31) Guengerich, F. P., and Kim, D.-H. (1991) Enzymatic oxidation of ethyl carbamate to vinyl carbamate and its role as an intermediate in the formation of 1,N^6-ethenoadenosine. *Chem. Res. Toxicol.* **4**, 413−421.
(32) Guengerich, F. P., and Böcker, R. H. (1988) Cytochrome P-450-catalyzed dehydrogenation of 1,4-dihydropyridines. *J. Biol. Chem.* **263**, 8168−8175.
(33) Vermeulen, N. P. E., Bessems, J. G. M., and Van de Straat, R. (1992) Molecular aspects of paracetamol-induced hepatotoxicity and its mechanism-based prevention. *Drug Metab. Rev.* **24**, 367−407.
(34) Teitelbaum, P. J., Chu, N. I., Cho, D., Tökés, L., Patterson, J. W., Wagner, P. J., and Chaplin, M. D. (1981) Mechanism for the oxidative defluorination of flunisolide. *J. Pharmacol. Exp. Ther.* **218**, 16−22.
(35) Vyas, K. P., Kari, P. H., Prakash, S. R., and Duggan, D. E. (1990) Biotransformation of lovastatin II. In vitro metabolism by rat and mouse liver microsomes and involvement of cytochrome P-450 in dehydrogenation of lovastatin. *Drug Metab. Dispos.* **18**, 218−222.
(36) Dinnocenzo, J. P., and Banach, T. E. (1989) Deprotonation of tertiary amine cation radicals. A direct experimental approach. *J. Am. Chem. Soc.* **111**, 8646−8653.
(37) Guengerich, F. P., Okazaki, O., Seto, Y., and Macdonald, T. L. (1995) Radical cation intermediates in *N*-dealkylation reactions. *Xenobiotica* **25**, 689−709.
(38) Karki, S. B., Dinnocenzo, J. P., Jones, J. P., and Korzekwa, K. R. (1995) Mechanism of oxidative amine dealkylation of substituted *N*,*N*-dimethylanilines by cytochrome P-450: application of isotope effect profiles. *J. Am. Chem. Soc.* **117**, 3657−3664.

TX9501187